Stripe-to-bubble transition of magnetic domains at the spin reorientation of (Fe/Ni)/Cu/Ni/Cu(001)

J. Wu,[1] J. Choi,[1] C. Won,[2] Y. Z. Wu,[3] A. Scholl,[4] A. Doran,[4] Chanyong Hwang,[5] and Z. Q. Qiu[1]
[1]*Department of Physics, University of California–Berkeley, Berkeley, California 94720, USA*
[2]*Department of Physics, Kyung Hee University, Seoul 130-701, Korea*
[3]*Surface Physics Laboratory (National Key Laboratory), Fudan University, Shanghai 200433, China*
[4]*Advanced Light Source, Lawrence Berkeley National Laboratory, Berkeley, California 94720, USA*
[5]*Division of Advanced Technology, Korea Research Institute of Standards and Science, 209 Gajeong-Ro, Yuseong-Gu, Daejeon 305-340, Korea*

(Received 21 October 2008; revised manuscript received 11 December 2008; published 22 January 2009)

Magnetic domain evolution at the spin reorientation transition (SRT) of (Fe/Ni)/Cu/Ni/Cu(001) is investigated using photoemission electron microscopy. While the (Fe/Ni) layer exhibits the SRT, the interlayer coupling of the perpendicularly magnetized Ni layer to the (Fe/Ni) layer serves as a virtual perpendicular magnetic field exerted on the (Fe/Ni) layer. We find that the perpendicular virtual magnetic field breaks the up-down symmetry of the (Fe/Ni) stripe domains to induce a net magnetization in the normal direction of the film. Moreover, as the virtual magnetic field increases to exceed a critical field, the stripe domain phase evolves into a bubble domain phase. Although the critical field depends on the Fe film thickness, we show that the area fraction of the minority domain exhibits a universal value that determines the stripe-to-bubble phase transition.

DOI: 10.1103/PhysRevB.79.014429 PACS number(s): 75.70.Ak

I. INTRODUCTION

Spin reorientation transition (SRT) (Refs. 1 and 2) refers to the phenomenon of spin directional change in magnetic materials due to the change in the so-called magnetic anisotropy. For example, in a magnetic thin film the competition between the perpendicular crystalline magnetic anisotropy and the in-plane magnetic shape anisotropy could switch the film magnetization from perpendicular to the in-plane directions of the film by changing the temperature or film thickness. Research on this subject has attracted great interest in the last decades because of its connection to the magnetic ordering in two-dimensional (2D) magnetic systems.[3,4] It is shown that the apparent loss of the macroscopic magnetization within a narrow gap of the temperature (or film thickness) at the SRT is due to the formation of magnetic stripe phase.[5] The stripe phase was also shown in experiment to exhibit unique dynamic properties.[6,7] The difficulty of applying a magnetic field in an electron microscope was also circumvented recently by doing element-specific domain imaging in a magnetic sandwich where the magnetic interlayer coupling serves as a virtual magnetic field.[8] In particular, the improvement of the sample fabrication quality greatly enhances the domain imaging quality,[9,10] making it possible to perform a quantitative analysis on the stripe domain width.[8] These advances in experiment enable a deeper probe of some mechanisms that govern the magnetic phases at the SRT. For example, it is shown that the exponential decay of the stripe width toward the SRT point is a manifest of a crossover from the anisotropy to the dipolar length scales and that a paramagnetic gap develops at the SRT point.[11,12] Recently, research on this subject has been focused on the search of new magnetic domain phases at the SRT under different conditions.[13,14] Because of the long-range character of the dipolar interaction, it is usually difficult for theory to predict the ground state of the magnetic phase. Thus computer simulation and special analytical solutions are usually employed to compare the energy of the stripe domain phase with the energy of other domain phases.[15–17] In experiment, a recent observation shows that after magnetizing a film with a magnetic field slightly tilting away from the film in-plane direction, the magnetic stripe phase of the film changes into a bubble domain phase.[18] This observation suggests that there could exist other domain phases in competition with the stripe domain phase at the SRT, and the ground state of a 2D magnetic system could be switched from the stripe phase to the bubble phase within a magnetic field. In this paper, we report a study of (Fe/Ni)/Cu/Ni(20 ML)/Cu(001) system in which the interlayer coupling between the perpendicular magnetized 20 ML Ni film and the (Fe/Ni) film serves as a virtual perpendicular magnetic field applied to the (Fe/Ni) film which undergoes the SRT. By doing element-specific magnetic domain imaging using photoemission electron microscopy (PEEM), we investigated the (Fe/Ni) stripe domain phase within a perpendicular magnetic field. We find a phase transition from the stripe phase to the bubble phase as the virtual magnetic field exceeds a critical field. Furthermore, we reveal that this stripe-to-bubble phase transition is determined by a universal value of the minority domain area fraction.

II. EXPERIMENT

A 10-mm-diameter Cu(001) single-crystal substrate was mechanically polished with 0.25 μm diamond past finish and electropolished as previously reported.[9] The Cu substrate was cleaned in an ultrahigh vacuum (UHV) system with a base pressure of 2×10^{-10} Torr by cycles of Ar ion sputtering at 1–5 keV and annealing at ~600 °C until sharp low energy electron diffraction (LEED) spots are observed. The sample of [Fe/Ni(5 ML)]/Cu/Ni(20 ML) was grown epitaxially onto the Cu(001) substrate by evaporating Fe, Ni, and

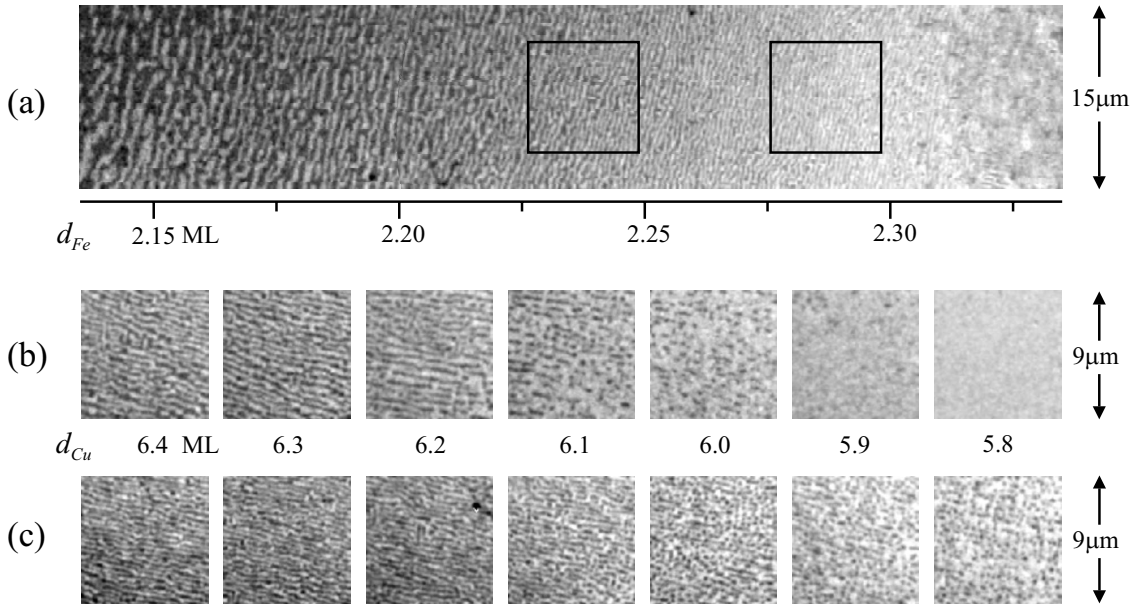

FIG. 1. (a) PEEM image of the Fe magnetic domains in Fe/Ni(5 ML)/Cu(6.40 ML)/Ni(20 ML)/Cu(001). $d^0_{Cu}=6.40$ ML corresponds to a zero interlayer coupling between the (Fe/Ni) film and the Ni(20 ML) film. The stripe domain width decreases with increasing the Fe film thickness toward the SRT point at $d^0_{Fe}=2.32$ ML, above which the Fe film has an in-plane magnetization. [(b) and (c)] PEEM images of the Fe domains at (b) $d_{Fe}=2.24$ and (c) 2.29 ML as a function of the Cu film thickness. The position of the first images of (b) and (c) are marked by the two boxes in figure (a) except the 90° rotation for a clearer view of the domain pattern evolution. Changing Cu thickness away from the zero coupling point of $d^0_{Cu}=6.40$ ML is equivalent to applying a virtual perpendicular magnetic field to the (Fe/Ni) film. The (Fe/Ni) magnetic stripe phase evolves into a bubble phase before being saturated.

Cu from thermal crucibles at an evaporation rate of ~1 Å/min. The Fe (0–5 ML) and Cu (0–15 ML) films were grown into cross wedges over 2 mm length along two orthogonal directions for the purpose of controlling their thicknesses independently.[9] The wedge is formed by moving the substrate behind a knife-edge shutter during the growth with the wedge slope derived from the moving speed and the evaporation rate. The sample was covered with a 10 ML Cu protective layer before being transferred into the PEEM chamber at beamline 7.3.1.1 at the Advanced Light Source. The x-ray beam was circularly polarized and incident at an angle of 60° to the surface-normal direction. The magnetic domain images were obtained by taking the ratio of L_3 and L_2 edges utilizing the effect of x-ray magnetic circular dichroism (XMCD). All measurements were made at room temperature.

The [Fe/Ni(5 ML)] bilayer behaves as a single ferromagnetic film because of the strong direct ferromagnetic coupling between the Fe and Ni magnetizations as previously reported.[8,9] The purpose of using a 5 ML Ni film is to shift the SRT thickness of the Fe/Ni into the ferromagnetic phase of fcc Fe so that the complicated ferromagnetic-to-antiferromagnetic transition of the fcc Fe at ~4 ML Fe is outside the SRT region of the Fe/Ni(5 ML).[8] In this paper, we show only Fe PEEM images to represent the (Fe/Ni) magnetic domains. It was shown that the interlayer coupling in a magnetic-coupled sandwich serves as a virtual magnetic field.[8,19] Then since 20 ML Ni on Cu(001) has a perpendicular magnetization,[20] the SRT of the (Fe/Ni) layer in the [Fe/Ni(5 ML)]/Cu/Ni(20 ML) system is equivalent to the SRT of a (Fe/Ni) film within a perpendicular magnetic field whose strength varies with the interlayer Cu thickness. At the PEEM beamline, prior to the PEEM measurement, the sample was magnetized in a 1 kOe magnetic field normal to the film surface to wipe out the magnetic domains of the 20 ML Ni film, ensuring a uniform exchange coupling between the Ni and the (Fe/Ni) films.

III. RESULT AND DISCUSSION

Figure 1 shows PEEM images of [Fe/Ni(5 ML)]/Cu/Ni(20 ML)/Cu(001) at 6.4 ML Cu where the interlayer coupling between the (Fe/Ni) and the Ni layers is zero. Then the Fe magnetic images should represent the (Fe/Ni) magnetic domains within a zero external magnetic field. Below $d^0_{Fe}=2.32$ ML, the (Fe/Ni) film exhibits a clear stripe domain phase with the stripe width decreasing rapidly with increasing the Fe film thickness. Above 2.32 ML of the Fe film thickness, the (Fe/Ni) film possesses irregular magnetic domains. After rotating the sample around its surface-normal direction by 90°, the domain contrast remains unchanged below 2.32 ML of Fe but changes above 2.32 ML of Fe, showing that the (Fe/Ni) magnetization is perpendicular to the film plane below 2.32 ML of Fe ($d_{Fe}<2.32$ ML) and parallel to the film plane above 2.32 ML of Fe ($d_{Fe}>2.32$ ML). Therefore, we identify $d^0_{Fe}=2.32$ ML to be the (Fe/Ni) SRT point. The domain phase of the out-of-plane Fe magnetization will be the focus for the rest of this paper. Another observation from Fig. 1(a) is that the up (white) and down (dark) magnetic stripes have equal width, which is expected because the up-down symmetry should not be broken in the absence of an external magnetic field.[9] Recalling

that the interlayer coupling between the (Fe/Ni) and the 20 ML Ni layers oscillates with the Cu spacer layer thickness,[21] the $d_{\mathrm{Cu}}^{0}=6.40$ ML actually defines the boundary between the antiferromagnetic interlayer coupling ($d_{\mathrm{Cu}}<6.40$ ML) and the ferromagnetic coupling ($d_{\mathrm{Cu}}>6.40$ ML) regions.[22,23] Thus the evolution of the stripe phase in the vicinity of $d_{\mathrm{Cu}}^{0}=6.40$ ML represents the stripe phase evolution as a function of a perpendicular magnetic field applied to the (Fe/Ni) film.

We find that increasing/decreasing the Cu thickness away from $d_{\mathrm{Cu}}^{0}=6.40$ ML results in the same domain evolution except for a reversal of the white and dark domains. This is expected because ferromagnetic and antiferromagnetic couplings correspond to applying a perpendicular magnetic field to the (Fe/Ni) film in the direction parallel and antiparallel to the 20 ML Ni magnetization, respectively, and thus should result in the same domain evolution after a reversal of the up-down direction (e.g., $H\rightarrow -H$). Because of the above fact and that synchrotron beam time is limited, we only focus on one side of the Cu thickness away from the zero coupling point of $d_{\mathrm{Cu}}^{0}=6.40$ ML to obtain high-quality domain images. In this paper, we will focus on the $d_{\mathrm{Cu}}<6.40$ ML region where we optimized the PEEM operation condition to obtain a good spatial resolution of the domain images. Figures 1(b) and 1(c) show a series of Fe domain images as a function of the Cu film thickness for two representative stripe domains at $d_{\mathrm{Fe}}=2.24$ and 2.29 ML, respectively [the areas boxed in Fig. 1(a)]. As the Cu thickness varies away from the zero coupling point of $d_{\mathrm{Cu}}^{0}=6.40$ ML, the interlayer coupling strength increases (or the virtual magnetic field strength increases). We find that the majority (white) domain area expands at the cost of shrinking the minority (dark) domain area, i.e., a net magnetization of the (Fe/Ni) film, which is proportional to the area difference between the majority and minority domains that increases with the interlayer coupling strength. This is expected because a perpendicular magnetic field, which is simulated here by the interlayer coupling, should break the up-down domain symmetry to induce a net perpendicular magnetization. The interesting observation of the PEEM images is that as the magnetization increases with the interlayer coupling, the stripe domain phase also evolves in a manner where the minority (dark) stripes break at a point to develop a bubble domain phase [$d_{\mathrm{Cu}}<6.1$ ML for Fig. 1(b) and $d_{\mathrm{Cu}}<6.0$ ML for Fig. 1(c)]. Despite the difference of the Cu thickness where the bubble domain phase appears, measurement at other Fe thicknesses confirms the fact that the stripe phase evolves into the bubble phase above a critical value of the interlayer coupling strength (or equivalently speaking, above a critical value of the perpendicular magnetic field). Another interesting observation is that the majority (white) domain width and area increase with the virtual perpendicular magnetic field, but the width of the minority (black) domains changes very little regardless if it is in the stripe phase or in the bubble phase.

To better understand the stripe-to-bubble phase transition, we performed the following quantitative analysis of the PEEM images in Figs. 1(b) and 1(c). First, we analyzed the dependence of the perpendicular magnetization (M) of the (Fe/Ni) film on the perpendicular magnetic field (H). Since the magnetization is linearly proportional to the area difference of the majority and minority domains, it is obvious that the normalized magnetization M/M_S, where M_S is the saturation magnetization, is determined by the area fraction (f) of the minority domains in the form of $M/M_S=1-2f$. Thus we determine the (Fe/Ni) normalized magnetization M/M_S by calculating the minority domain area fraction of the PEEM images at different Cu thicknesses. Second, we assume that the interlayer coupling strength, which simulates the perpendicular magnetic field, in the vicinity of zero coupling is linearly proportional to the Cu thickness difference away from the zero coupling point [$H\propto \delta d_{\mathrm{Cu}}\equiv |d_{\mathrm{Cu}}-d_{\mathrm{Cu}}^{0}|$]. Therefore Fig. 2 actually represents the result of the normalized magnetization M/M_S versus a perpendicular magnetic field for the domain images of Figs. 1(b) and 1(c). In both cases, the M/M_S increases monotonically with δd_{Cu} toward its saturation. The different slopes of the M/M_S vs δd_{Cu} reflect the fact of different saturation magnetic field at the two Fe film thicknesses. This result is not surprising because a film closer to the SRT point should have a weaker overall perpendicular magnetic anisotropy thus a greater saturation magnetic field in the perpendicular direction. The stripe-to-bubble phase transition, however, does not generate any abnormal behavior of the M/M_S-δd_{Cu} curve, showing that the domain pattern change does not produce any obvious discontinuity in the macroscopic magnetization. Another result of Figs. 1 and 2 is that the stripe-to-bubble phase transition occurs at different δd_{Cu} for the two Fe film thicknesses, indicating that this stripe-to-bubble domain transition depends on both the perpendicular magnetic field and the magnetic anisotropy.

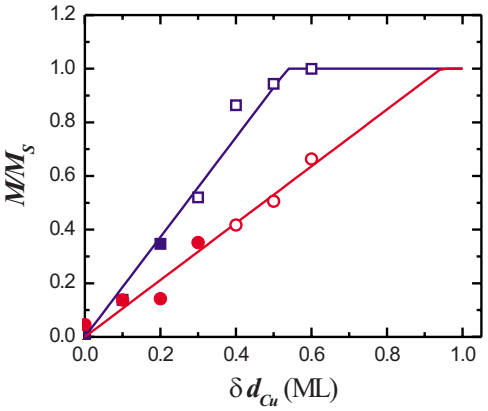

FIG. 2. (Color online) The normalized magnetization M/M_S determined from PEEM images as a function of $\delta d_{\mathrm{Cu}}=|d_{\mathrm{Cu}}-d_{\mathrm{Cu}}^{0}|$ which simulates the strength of the perpendicular virtual magnetic field applied to the (Fe/Ni) film. Data from $d_{\mathrm{Fe}}=2.24$ ML [Fig. 1(b)] are represented by square symbols; data from $d_{\mathrm{Fe}}=2.29$ ML [Fig. 1(c)] are represented by circular symbols. Solid symbols represent the stripe phase and open symbols represent the bubble phase. The solid lines are guides for the eyes.

The result of Figs. 1 and 2 shows that although the macroscopic magnetization does not show any anomaly in response to a perpendicular magnetic field within the SRT region, the magnetization process is accompanied by two types of distinguishable magnetic domain phases. (1) At low field, M/M_S increases with H in a manner of retaining the stripe domain phase. (2) Above a critical field, the minority stripes

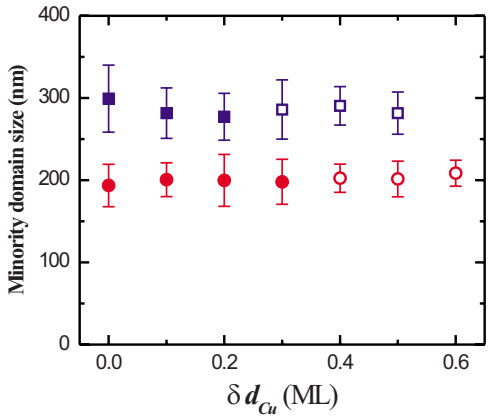

FIG. 3. (Color online) The minority domain size as a function of δd_{Cu}. Data from $d_{\mathrm{Fe}}=2.24$ ML [Fig. 1(b)] are represented by square symbols; data from $d_{\mathrm{Fe}}=2.29$ ML [Fig. 1(c)] are represented by circular symbols. Solid symbols represent the stripe phase and open symbols represent the bubble phase.

start to break to evolve into a bubble domain phase. Noticing that the M/M_S is proportional to the area difference between the majority and minority domains, we should focus our attention on the domain size change during the magnetization process. As shown in Figs. 1(b) and 1(c), the majority (white) domain area increases with H but its domain size becomes ill defined especially after the majority stripes merge together. On the other hand, the minority (dark) domain size can be reliably determined from the PEEM images so that we determine and plot the minority domain size as a function of δd_{Cu} in Fig. 3. Here the minority domain size is defined as the stripe width in the stripe phase or the bubble diameter in the bubble phase. It is clear from Fig. 3 that the minority domain size remains roughly a constant with increasing the δd_{Cu} despite the increased M/M_S and the stripe-to-bubble phase transition. Combining the information from Figs. 2 and 3, we summarize the microscopic scenario of the

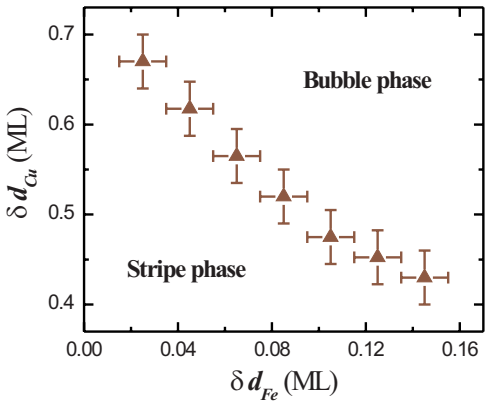

FIG. 4. (Color online) Phase diagram of the magnetic domains in the δd_{Fe}-δd_{Cu} plane. Here $\delta d_{\mathrm{Fe}} \equiv |d_{\mathrm{Fe}} - d^0_{\mathrm{Fe}}|$, where $d^0_{\mathrm{Fe}}=2.32$ ML is the SRT point, is proportional to the perpendicular magnetic anisotropy and $\delta d_{\mathrm{Cu}} \equiv |d_{\mathrm{Cu}} - d^0_{\mathrm{Cu}}|$, where $d^0_{\mathrm{Cu}}=6.40$ ML is the zero interlayer coupling point, is proportional to the virtual perpendicular magnetic field applied to the (Fe/Ni) SRT film. The boundary between the stripe and bubble phases is marked by the triangle symbol.

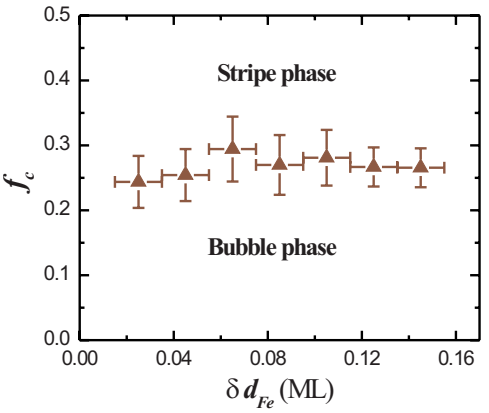

FIG. 5. (Color online) Critical area fraction f_c as a function of δd_{Fe}. The independence of f_c on δd_{Fe} shows that it is the area fraction f that determines the stripe-to-bubble phase transition.

magnetization process as the following. At low magnetic field, the majority stripe width expands while the minority stripe width remains unchanged. Above a critical field, the minority stripes break into bubbles to further shrink the minority domain area while keeping the bubble domain size unchanged. It should be pointed out that the unchanged minority domain size shows that the magnetization of the film must take place by annihilating the minority stripes at low field. Unfortunately we cannot reveal this process because it requires the imaging of the same area within a magnetic field.

The appearance of the bubble domain phase in the magnetization process needs more analysis, especially on why the bubble domain phase appears above a critical magnetic field. Figures 1(b) and 1(c) show that the critical magnetic field (or δd_{Cu}), where the bubble domain phase appears, depends on the perpendicular magnetic anisotropy (or $\delta d_{\mathrm{Fe}} \equiv |d_{\mathrm{Fe}} - d^0_{\mathrm{Fe}}|$, where $d^0_{\mathrm{Fe}}=2.32$ ML is the SRT point). We identified the stripe-to-bubble phase-transition position from the PEEM images and plot the stripe/bubble phase boundary in the δd_{Fe}-δd_{Cu} plane (Fig. 4). Figure 4 displays a clear dependence of the critical field (or δd_{Cu}) on the magnetic anisotropy (or δd_{Fe}), showing that neither the critical field nor the magnetic anisotropy alone determines the stripe-to-bubble phase transition. In an effort to find a universal behavior underlying the stripe-to-bubble phase transition, we determined the area fraction f_C of the minority domains at the stripe-to-bubble transition boundary and plot the result in the f-δd_{Fe} plane (Fig. 5). In this plane, the critical area fraction f_C separates the stripe and the bubble phases for each δd_{Fe}. Then we find an important result from Fig. 5 that this critical area fraction f_C is *independent* of the δd_{Fe}, showing that it is the area fraction f that determines the stripe-to-bubble phase transition. Taking into account the thickness variation, we can draw a conclusion that the ground state of the (Fe/Ni) domains is in the stripe phase for $f<0.2$ and in the bubble phase for $f>0.3$ with $0.2<f<0.3$ being the transition region between these two phases.

At the end, we discuss some existing theories relating to the stripe phase within a perpendicular magnetic field. The appearance of the magnetic domains in the SRT region is a

result of the competition among the long-range dipole interaction, the short-range magnetic exchange interaction, and the on-site magnetic anisotropy. Specifically, the exponential decrease in the stripe width toward a minimum value at the SRT point is a result of an anisotropy-to-dipole length scale crossover.[11] For a 2D Heisenberg system consisting of a uniaxial magnetic anisotropy, the stripe domain evolution as a function of a perpendicular magnetic field has been addressed theoretically in the region where the stripe width is much greater than the minimum domain width (or where the anisotropy length governs the magnetic order). The result shows that the increased magnetization in response to a perpendicular magnetic field is realized by expanding the majority stripe width.[24] However, the theory also predicts that the minority stripe width should remain a finite value even as the macroscopic magnetization approaches its saturation. Although it is not justified to apply the above theory directly to the regime close to the SRT point (the case in our experiment or the regime where the dipole length governs the magnetic order),[11] the unchanged minority domain width in our experimental observation is to a certain degree captured by the above theory. This result was also evidenced in previous experiments, although the relative poor sample quality produces large fluctuations in the minority domain width.[9,10] On the other hand, the appearance of the bubble domain phase reported in the present paper is certainly not included in previous theories and experiments.

Another simplified model considers only the domain-wall energy and the dipole interaction energy.[25] Since both energy terms depend on specific domain patterns, the model compared the total energy of stripe phase and bubble phase within a perpendicular magnetic field. By changing the domain pattern from stripe phase into bubble phase, the increased domain-wall energy due to the increased domain-wall length is accompanied by a decrease in the dipole interaction energy. Thus the final domain state will depend on the competition between the above two terms. By a numerical simulation, the model shows that although the magnetization (or area fraction f) depends little on the domain patterns, the stripe- and bubble-phase energies do cross as a function of the minority area fraction, leading to a lower energy for stripe phase for $f>0.28$ and a lower energy for bubble phase for $f<0.28$. This result agrees well with our experimental observation. Reference 25 further predicts that in the vicinity of $f_c=0.28$, the system should process a phase separation into a superposition of stripe and bubble domain phases in a narrow region around f_c. This also agrees with our observation that the stripe and bubble domains coexist in the vicinity of the stripe-to-bubble phase-transition boundary. Although this simplified model explains the appearance of the bubble domain phase within a perpendicular magnetic field, the model ignores the magnetic anisotropy term. We wish that future theoretical study could be carried out to directly address our experimental observation.

IV. SUMMARY

In summary, we studied the domain evolution of (Fe/Ni) film at the SRT in (Fe/Ni)/Cu/Ni/Cu(001) where the interlayer coupling simulates a virtual perpendicular magnetic field applied to the (Fe/Ni) film. We find that as the magnetic field increases, the (Fe/Ni) magnetization initially increases by increasing the majority domain area while keeping the minority stripe width unchanged, and then above a critical magnetic field the minority stripes break to evolve into a bubble domain phase. We further show that although the critical field depends on the magnetic anisotropy, a universal value of the minority domain area fraction ($f_C \sim 0.2-0.3$) determines the stripe-to-bubble phase transition.

ACKNOWLEDGMENTS

This work was supported by National Science Foundation under Grant No. DMR-0803305, U.S. Department of Energy under Grant No. DE-AC02-05CH11231, National Natural Science Foundation of China 973-Project under Grant No. 2006CB921300, ICQS Chinese Academy of Sciences, and KICOS through Global Research Laboratory project.

[1] D. P. Pappas, K. P. Kämper, and H. Hopster, Phys. Rev. Lett. **64**, 3179 (1990).
[2] Z. Q. Qiu, J. Pearson, and S. D. Bader, Phys. Rev. Lett. **70**, 1006 (1993).
[3] N. D. Mermin and H. Wagner, Phys. Rev. Lett. **17**, 1133 (1966).
[4] Myron Bander and D. L. Mills, Phys. Rev. B **38**, 12015 (1988).
[5] R. Allenspach and A. Bischof, Phys. Rev. Lett. **69**, 3385 (1992).
[6] O. Portmann, A. Vaterlaus, and D. Pescia, Nature (London) **422**, 701 (2003).
[7] O. Portmann, A. Vaterlaus, and D. Pescia, Phys. Rev. Lett. **96**, 047212 (2006).
[8] Y. Z. Wu, C. Won, A. Scholl, A. Doran, H. W. Zhao, X. F. Jin, and Z. Q. Qiu, Phys. Rev. Lett. **93**, 117205 (2004).
[9] H. J. Choi, W. L. Ling, A. Scholl, J. H. Wolfe, U. Bovensiepen, F. Toyama, and Z. Q. Qiu, Phys. Rev. B **66**, 014409 (2002).
[10] G. Meyer, T. Crecelius, A. Bauer, I. Mauch, and G. Kaindl, Appl. Phys. Lett. **83**, 1394 (2003).
[11] C. Won, Y. Z. Wu, J. Choi, W. Kim, A. Scholl, A. Doran, T. Owens, J. Wu, X. F. Jin, H. W. Zhao, and Z. Q. Qiu, Phys. Rev. B **71**, 224429 (2005).
[12] M. Carubelli, O. V. Billoni, S. A. Pighín, S. A. Cannas, D. A. Stariolo, and F. A. Tamarit, Phys. Rev. B **77**, 134417 (2008).
[13] J. H. Gao, Y. Girard, V. Repain, A. Tejeda, R. Belkhou, N. Rougemaille, C. Chacon, G. Rodary, and S. Rousset, Phys. Rev. B **77**, 134429 (2008).
[14] J. P. Whitehead, A. B. MacIsaac, and K. DeBell, Phys. Rev. B **77**, 174415 (2008).
[15] A. B. MacIsaac, K. De'Bell, and J. P. Whitehead, Phys. Rev. Lett. **80**, 616 (1998).
[16] E. Y. Vedmedenko, H. P. Oepen, A. Ghazali, J.-C. S. Lévy, and J. Kirschner, Phys. Rev. Lett. **84**, 5884 (2000).
[17] A. P. Popov, N. V. Skorodumova, and O. Eriksson, Phys. Rev. B

77, 014415 (2008).
[18] J. Choi, J. Wu, C. Won, Y. Z. Wu, A. Scholl, A. Doran, T. Owens, and Z. Q. Qiu, Phys. Rev. Lett. **98**, 207205 (2007).
[19] K. Mandal, S. P. Mandal, M. Vázquez, S. Puerta, and A. Hernando, Phys. Rev. B **65**, 064402 (2002).
[20] P. J. Jensen, K. H. Bennemann, P. Poulopoulos, M. Farle, F. Wilhelm, and K. Baberschke, Phys. Rev. B **60**, R14994 (1999).
[21] S. S. P. Parkin, N. More, and K. P. Roche, Phys. Rev. Lett. **64**, 2304 (1990).
[22] Z. Q. Qiu, J. Pearson, and S. D. Bader, Phys. Rev. B **46**, 8659 (1992).
[23] R. K. Kawakami, E. Rotenberg, Ernesto J. Escorcia-Aparicio, Hyuk J. Choi, J. H. Wolfe, N. V. Smith, and Z. Q. Qiu, Phys. Rev. Lett. **82**, 4098 (1999).
[24] Ar. Abanov, V. Kalatsky, V. L. Pokrovsky, and W. M. Saslow, Phys. Rev. B **51**, 1023 (1995).
[25] Kwok-On Ng and David Vanderbilt, Phys. Rev. B **52**, 2177 (1995).